

# Assessment of Time Effects on Compressive Bearing Capacity of Steel Pipe Piles Driven in Clay Deposits of Persian Gulf

Amir Hossein Shamshirgaran <sup>1</sup>, Babak Ebrahimian <sup>2\*</sup>

<sup>1</sup> Graduate Master Student in Geotechnical Engineering, Faculty of Civil, Water and Environmental Engineering, Shahid Beheshti University, Tehran, Iran; [shamshirgaran.amir@gmail.com](mailto:shamshirgaran.amir@gmail.com)

<sup>2</sup> Assistant Professor, Department of Geotechnical and Transportation Engineering, Faculty of Civil, Water and Environmental Engineering, Shahid Beheshti University, Tehran, Iran; [b\\_brahimian@sbu.ac.ir](mailto:b_brahimian@sbu.ac.ir)

## ARTICLE INFO

### Article History:

Received: 22 Jun. 2021

Accepted: 02 Jan. 2022

### Keywords:

Offshore pile

Bearing capacity

CPTu

PDA test

Time function

Set-up

## ABSTRACT

Offshore oil and gas extraction structures at shallow waters are conventionally supported by long driven steel pipe piles. In recent years, the direct CPT- or CPTu-based pile design methods have broadly been used to predict the bearing capacity of offshore piles in a more reliable manner. On the other hand, previous investigations have shown that the pile capacity is time-dependent (set-up and relaxation phenomena). However, time effects are missing in most CPT- or CPTu-based prediction methods. The main objective of this paper is to estimate the axial compressive bearing capacity of the offshore steel pipe piles driven in the marine clay deposits of the Persian Gulf based on some popular CPT/CPTu as well as static -based prediction methods. The estimated results are compared with the measured capacities obtained from the Pile Dynamic Analyzer (PDA) and the Case Pile Wave Analysis Program (CAPWAP). The measured values have been recorded at End-Of-Drive (EOD) and Beginning-Of-Restrike (BOR) conditions periodically up to nine months after pile installation. Then, the most reliable bearing capacity prediction methods are determined based on the shaft, base, and ultimate capacity values in short, medium, and long-term conditions. Here, five open-ended long steel pipe piles driven into very soft to hard marine clays of the Persian Gulf, Iran are considered to verify and evaluate the prediction quality of each method. It is shown that the ratio of predicted to measured ultimate bearing capacities obtained from the static analysis methods averagely have around 64% more scattering than the corresponding values obtained from the CPT and CPTu-based methods. The results of the current investigation can be employed in offshore piling projects of the Persian Gulf in which the time constraints of installation do not allow running dynamic load tests at different time intervals.

## 1. Introduction

Cone penetration test (CPT) is vastly employed in the design of offshore piles. The reliability, high-quality results and continuous recording of soil resistance in depth are the CPT advantages which result in excellent performance of CPT rather than the other in-situ tests. Moreover, the shapes of CPT and pile as well as their failure mechanisms developed during penetration process are similar. These salient features have motivated many researchers to propose direct pile bearing capacity estimation methods using CPT data. One of the main geotechnical challenges of driven piles is the variation of their bearing capacities with time. It has been well-accepted that the bearing capacity of driven prefabricated piles may increase (set-up) or

decrease (relaxation) with time depending on the soil type [1, 2]. In this regard, the variation of bearing capacity has been observed to be rapid at the onset, but its rate substantially decreases with the elapse of time [3]. Set-up phenomenon was first documented in non-cohesive soils [1]. Subsequently, a number of other set-up case histories were also reported by other researchers [4-6]. They collectively show that set-up is more predominant in fine-grained cohesive soils rather than the other soil types. The main causes of soil set-up can be categorized into the following groups [7]:

1. *Dissipation of excess pore water pressures (EPWP) due to pile installation:* Pile driving in clay produces large changes in total stresses and pore water pressures in its surroundings. The excess pore water

pressures will dissipate in time as a result of the subsequent reconsolidation of clayey soils. This leads to an increase of horizontal effective stresses acting on the pile shaft implying an increase of mobilized skin friction along the pile with time.

2. *Ageing*: The pile capacity increase starting after the end of reconsolidation phase may be due to the changes of soil skeleton characteristics, pile-soil interaction and/or stress regime in the soil medium surrounding a driven pile. For piles driven in clay, the changes of thixotropy, cementation or bonding of clay particles with time also play important roles.

According to [8], the soil set-up can be divided into three phases as shown in Fig. (1). Phase 1 shows the logarithmically nonlinear rate of the excess pore water pressure dissipation. Phase 2 indicates the logarithmically linear rate of the excess pore water pressure dissipation. Finally, the ongoing increase of the pile capacity over time at a linear but lower rate is introduced as the ageing in Phase 3. The soil set-up mechanism is illustrated in Fig. (1), where  $t$  is the time elapsed after initial driving, and  $t_0$  is the time when Phase 2 begins;  $Q_{initial}$  is the initial capacity, and  $Q_t$  is the final capacity corresponding to time  $t$ .

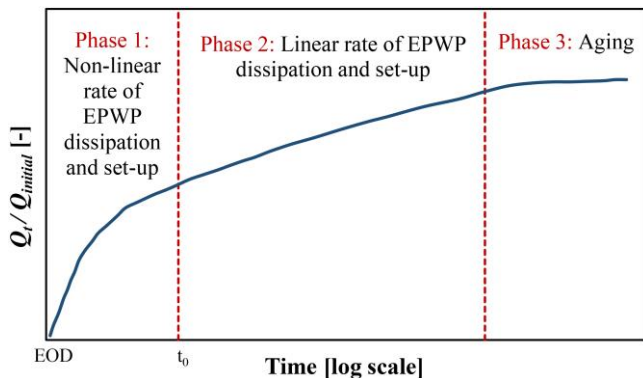


Fig. 1. Variation of soil set-up with time.

During the first phase, set-up is nonlinear with the logarithm of the time. This phenomenon is possibly attributed to the non-constant rate of the excess pore water dissipation, or other mechanisms that are complicated and have not been well understood yet. The duration of the first nonlinear phase, corresponding to the time parameter  $t_0$  in the predictive models, is a function of soil and pile properties [9-12]. In the second phase, set-up rate corresponds to the rate of excess pore water pressure dissipation. During the logarithmically constant rate of dissipation, the affected soil experiences an increase in effective vertical and horizontal stresses, and consolidates according to the conventional consolidation theory. The duration of this phase also depends on the soil and pile properties. In granular materials, full pore water pressure dissipation is expected to be taken place within a few hours after pile installation. In cohesive soils, however, dissipation may continue for several weeks, several months, or even several years [9, 13, 14]. During the third phase, set-up rate is independent of the effective stress, which

is known as soil ageing. This effect also leads to an increase in soil shear stiffness and dilatant behavior [15]. For cohesive soils, the majority of set-up is related to the dissipation of excess pore water pressure (i.e., the summation of Phase 1 and Phase 2) [16]. For granular soils, however, set-up is predominately associated with Phase 3 (i.e., ageing effect) due to relatively rapid dissipation of excess pore water pressure [10, 15].

To quantitatively evaluate the soil set-up in driven piles, most engineers use static and dynamic loading tests. It should be noted that Static Pile Loading Test (SPLT) and Pile Dynamic Analyzer test (PDA) only measure the pile load–displacement relation and ultimate load at the time of testing; they do not provide any information on pile capacity variations over the time. SPLTs must be repeated at different times after pile driving to evaluate any set-up effects (at least in two times; immediately and the possible longest time after driving), which can be time-consuming and costly during pile installation, particularly in offshore environment [14]. Therefore, it is essential to develop empirical and numerical solutions to enable analyzing and estimating long-term set-up effects on the basis of the limited numbers of SPLT and PDA results. In this regard, the pile bearing capacity calculation methods taking into account the time effects, shall be more favorable for engineers from the design point of view. In offshore environment, PDA testing equipment provides such a capability [17]. The main advantage of PDA test is the possibility of the capacity measurement at various time intervals, for example End-of-Drive (EOD) and at a certain time after the initial drive, which is the so-called Beginning of Restrike (BOR).

This paper focuses on several determinant questions: (1) Which of the End-Of-Drive (EOD) or Beginning of Restrike (BOR) values is more precisely correlated with the results of the CPT/CPTu -based prediction methods? (2) Which CPT/CPTu -based prediction method is more consistent with the PDA results in long term condition? (3) Which of the shaft or base resistances of the pile experiences more alteration after time elapses? Thus, the main objective of this paper is to compare the results of CPT/CPTu–based prediction methods with the PDA records at both EOD and BOR conditions, obtained from the results of test piles driven in offshore clays of the Persian Gulf, Iran. It is worth noting that the results of PDA tests at long-term condition in the offshore environments are very rare and usually unavailable. Therefore, the analytical outcomes of this study can provide further insights for the geotechnical designers involved in offshore piling projects regarding the long-term capacity of the offshore piles in the Persian Gulf region.

## 2. Studied Area

### 2.1. Field Tests

In this study, the information of five boreholes, named BH-1 to BH-5, including soil engineering parameters,

CPTu results at the vicinity of five long driven offshore test piles, named TP-1 to TP-5, has been utilized. The piles are the foundations of the fixed offshore oil and gas platforms (jackets) installed in the Persian Gulf. Fig. (2) shows the approximate location of the test piles. The geographical coordinates and the geometrical characteristics of each test pile have been summarized in Table 1. The dynamic pile testing program on each pile has been conducted in such a way that the end of driving (EOD), short, medium and long-term bearing capacity values can be achieved. Additionally, CPTu soundings have been carried out at the test piles locations, and their results are employed to calculate the axial compressive bearing capacity of offshore piles using the available CPT, CPTu and static based prediction methods.

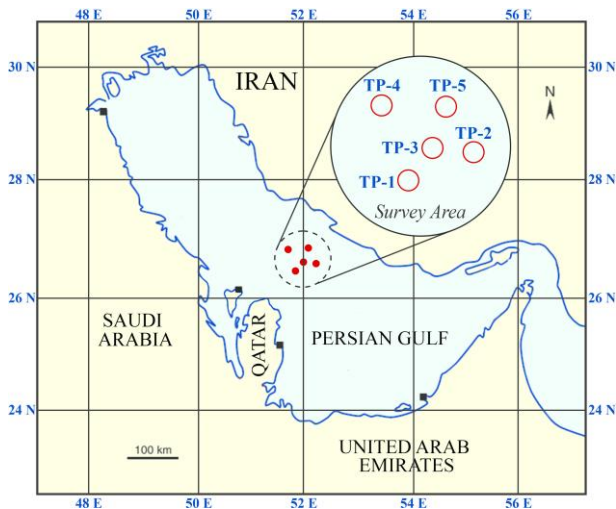


Fig. 2. Test piles locations in the Persian Gulf, south-west of Iran.

**2.2. Subsurface Condition**

In-situ piezocone penetration tests have been conducted; and the soil samples have also been obtained from the drilled boreholes adjacent to the location of piles to perform the laboratory tests. Figs. (3 & 4) show the relevant CPT records data and soil properties at the test pile TP-3. According to Fig. (3), the profiles have an increasing trend with depth; however, the values fluctuate in some occasional cohesionless granular lenses. In the considered area,

the clayey soil is very soft at above 20 m depth, stiff at 20–70 m depth, and very stiff to hard beyond 70 m depth. This layering pattern is dominant and no considerable variation is seen in the entire area [18].

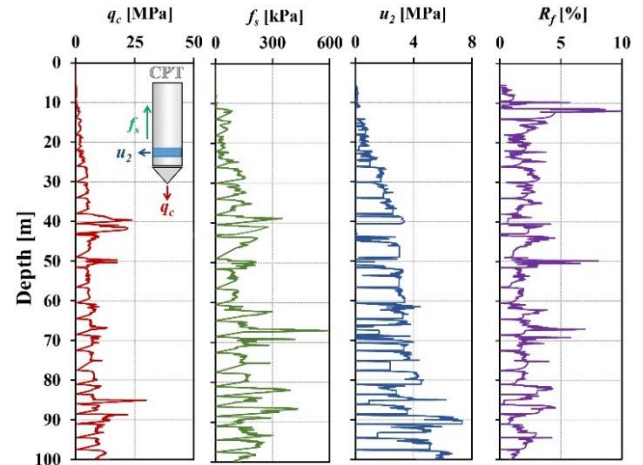


Fig. 3. CPTu profiles at the location of test pile TP-3.

Fig. (4) shows the soil profile as well as some typical mechanical properties obtained from laboratory tests conducted at various depths adjacent to the location of test pile TP-3. In this regard, undrained shear strength ( $S_u$ ), over consolidation ratio ( $OCR$ ) and plasticity index ( $I_p$ ) have been determined by UU triaxial, oedometer and Atterberg limits tests, respectively.

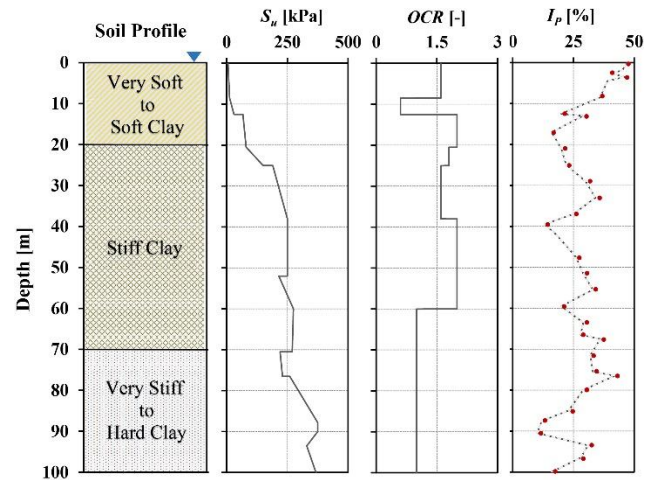


Fig. 4. Soil profile and mechanical properties at the location of test pile TP-3.

**Table 1. The geographical coordinates, geometrical characteristics of the test piles and PDA testing times.**

Bore-hole	Test Pile	Coordinate		Embedded Length [m]	Diameter (Thickness) [mm]	Water Depth [m]	PDA Testing Time [day]	Hammer Type (Weight [ton], Length [m])
		Latitude (N)	Longitude (E)					
BH-1	TP-1	26° 53' 37.114"	52° 12' 07.478"	101.10	1524 (50.80)	59.00	0 <sup>1</sup> , 15	IHC S600 <sup>3</sup> (65, 12.75)
BH-2	TP-2	26° 51' 01.484"	52° 11' 41.048"	106.50	1524 (50.80)	61.04	0, 35	
BH-3	TP-3	26° 51' 07.545"	52° 13' 49.447"	92.80	1524 (50.80)	73.89	0, 0.88 <sup>2</sup> , 9, 263	MHU 500T <sup>4</sup> (54.2, 11.80)
BH-4	TP-4	26° 53' 50.161"	52° 14' 15.487"	107.70	1524 (50.80)	61.04	0, 30, 45	
BH-5	TP-5	26° 47' 04.807"	52° 16' 52.927"	94.30	1524 (50.80)	61.59	0, 60	

Note: <sup>1</sup> End of Driving (EOD), <sup>2</sup> 21 hours after initial end of driving, <sup>3</sup> Maximum Energy = 600 kJ, <sup>4</sup> Maximum Energy = 550 kJ

### 2.3. Dynamic Pile Testing Program

In this research, in order to evaluate the predictive performance and applicability of different methods in determining the axial compressive bearing capacity of offshore piles in marine clayey soils of the Persian Gulf, 13 dynamic load tests are performed on the five test piles by a Pile Driving Analyzer (PDA) in various time intervals. As illustrated in Table 1, the testing times include initial driving (EOD) and restrike driving at approximately 21 hours, 9, 15, 30, 35, 45, 60 and 263 days after EOD. Accordingly, out of 13 dynamic tests performed on the piles, the bearing capacities of five cases have been measured immediately at EOD, two cases from a few hours to 10 days (short term), five cases from 10 days to 60 days (medium term) and one case after 263 days (long term). Signal matching analyses are conducted on the obtained field data by Case Pile Wave Analysis Program (CAPWAP). CAPWAP is a signal matching software program that uses pile top force and velocity measurements collected by PDA to extract the pile external forces. This software is applied to provide data on strain or force and acceleration, velocity or displacement of a pile under impact loading. The obtained data is then employed to estimate the bearing capacity and integrity of the pile, as well as the hammer performance, the pile stresses and the soil dynamic characteristics such as damping and quake factor values. This approach progresses by iterations to curve-fit the pile response determined in the wave equation model to the measured response of the actual pile during each hammer blow. The measured acceleration is used as an input to the pile model and afterward reasonable predictions are made for the soil resistance, quake, and damping factors. The force-time signal at the pile head is calculated using a wave equation program and compared to the measured force-time signal. The input parameters, including the soil-resistance distribution, quake, and damping are modified until the match between the measured and the calculated signals is deemed satisfactory. In this study, the applied values of quake and damping factors are in the range of 2.2 to 4.4 mm and 0.2 to 1, respectively.

The results of measured mobilized shaft, base, and ultimate bearing capacities,  $Q_m$ , are presented in Fig. (5). This figure indicates that shaft, base, and ultimate pile bearing capacities continually increase during 263-day period after initial driving due to the soil set-up effect. However, this effect is more pronounced in shaft comparing to base resistance. As it may be seen, the base resistance of the test piles only increases about 1.5 times, while the shaft resistance rises up to around 4.5 times after 263 days. It seems that shaft capacity varies considerably with time due to more engaged area of the pile skin rather than the pile base.

### 3. Prediction of Pile Axial Compressive Bearing Capacity

The ultimate axial load carrying capacity of pile ( $Q_u$ ) composed of the pile base capacity ( $Q_b$ ) and the pile shaft capacity ( $Q_s$ ). Pile weight is subtracted for piles in compression. The general equation is usually described by [19]:

$$Q_u = Q_s + Q_b = P_{out} \int q_s dz + q_b A_b \quad (1)$$

where  $P_{out}$  is the pile outer perimeter,  $q_s$  is the unit shaft resistance,  $q_b$  is the unit base resistance, and  $A_b$  is the cross section area of the pile base.

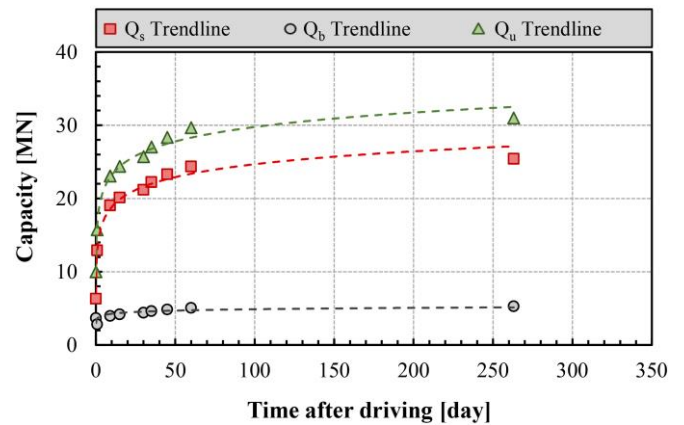


Fig. 5. Variation of shaft, base, and ultimate bearing capacities versus time for the test piles.

The ultimate bearing capacity of open-ended piles consist of two components similar to Eq. (1). However, the base capacity is produced by the sum of annulus capacity,  $Q_{ann}$  and plug capacity,  $Q_{plug}$ , presented in Eq. (2). The plug capacity is the minimum of inner shaft capacity,  $Q_{s,inn}$ , or soil base capacity,  $Q_{b,soil}$ , given in Eq. (4). The plug capacity is significantly influenced by the degree of soil plugging. Correspondingly, the degree of soil plugging depends on a number of major factors including the relative density of soil, the inner diameter and embedment of the pile.

$$Q_b = Q_{ann} + Q_{plug} \quad (2)$$

$$Q_{ann} = q_b A_b A_r \quad (3)$$

$$Q_{plug} = \min [Q_{s,inn}, Q_{b,soil}] \quad (4)$$

$$Q_{s,inn} = P_{inn} \int q_s dz \quad (5)$$

$$Q_{b,soil} = q_b A_b (1 - A_r) \quad (6)$$

$$A_r = 1 - \left( \frac{d}{D} \right)^2 \quad (7)$$

where  $P_{inn}$  is the pile inner perimeter,  $A_r$  is the pile area ratio, and finally,  $d$  and  $D$  are the inner and outer diameters of the pile, respectively.

During the last decades, several methods have been proposed to predict the pile capacity from CPT/CPTu data. These methods can be classified into the following groups [17]:

1. *Direct approach*: The unit base resistance,  $q_b$ , is computed from the cone tip resistance,  $q_c$ , and the shaft resistance,  $q_s$ , is obtained from either the sleeve friction,  $f_s$ , or  $q_c$  profiles.
2. *Indirect (Rational) approach*: The CPT data,  $q_c$  and  $f_s$ , are first used to calculate the soil shear strength parameters, such as the undrained shear strength,  $S_u$ , and the angle of internal friction,  $\phi$ . These parameters are then employed to obtain the values of  $q_b$  and  $q_s$ , using the formulas derived from the semi-empirical or theoretical relations.

In the current research, only the direct predicting methods of pile bearing capacity from the cone penetration test data are taken into account.

Additionally, the static analysis methods, for piles in clay, can be categorized to  $\alpha$ -method,  $\beta$ -method or  $\lambda$ -method. The skin friction is determined as follows [19]:

1. *Total stress approach ( $\alpha$ -method)*: The basic form of the total stress approach links the  $q_s$  to the average undrained shear strength,  $S_u$ , of clay along the pile shaft through an adhesion factor  $\alpha$ :

$$\alpha = q_s / S_u \quad (8)$$

2. *Effective stress approach ( $\beta$ -method)*: The effective stress approach is controlled by two dominant variables affecting the shaft capacity. They are the effective radial stress at failure,  $\sigma_{rf}'$ , and the frictional characteristics,  $\delta_f'$ , at the soil-pile interface:

$$\tau_f = \sigma_{rf}' \tan \delta_f' \quad (9)$$

$$\tau_f = k_f \sigma_{rf}' \tan \delta_f' \quad (10)$$

$$\beta = k_f \tan \delta_f' \quad (11)$$

Assuming that the effective radial coefficient at failure is equal to the at-rest radial stress coefficient, i.e.,  $k_f = k_0$ .

In order to assess the pile bearing capacity, herein, several direct CPT and CPTu -based methods as well as the static-based methods are employed. In this regard, the pile capacity prediction methods at the test piles locations are four property-based static analysis methods including API [20], FBV [21], NGI [22], and ICP [23] together with nine popular direct CPT and CPTu -based methods including Aoki & Velloso [24], Penpile [25], Shmertmann [26], de Ruiter & Beringen [27], Tumay & Fakhroo [28], Bustamanate & Gianeseli [29], Price & Wardle [30], Eslami & Fellenius [31], and Niazi & Mayne [32]. The details of the above prediction methods have been given in Table A1 in Appendix A. According to the literature, the time delay

between the initial pile driving and loading tests at different time elapses has not systematically been applied in CPT- and CPTu-based prediction methods. However, it has implicitly been taken into account for some methods such as UWA (2 to 68 days), NGI (100 days), ICP (50 days), and FBV (30 days).

Herein, the shaft, base, and ultimate bearing capacity curves obtained from different methods related to TP-3 are typically plotted in Fig. (6). The arithmetic average of the predicted shaft, base, and ultimate bearing capacities of TP-1 to TP-5 obtained from various methods are summarized in Table 2.

**Table 2. Average of the predicted shaft ( $Q_{s,ave}$ ), base ( $Q_{b,ave}$ ), and ultimate ( $Q_{u,ave}$ ) bearing capacities of the five test piles obtained from various methods.**

Method [Reference]	Type	$Q_{s,ave}$ [MN]	$Q_{b,ave}$ [MN]	$Q_{u,ave}$ [MN]
API [20]	Static	55.69	6.24	61.93
FBV [21]	Static	45.32	6.24	51.56
NGI [22]	Static	51.42	6.24	57.66
ICP [23]	Static	30.49	6.37	36.86
Aoki & Velloso [24]	CPT	45.12	4.29	49.41
Penpile [25]	CPT	13.07	2.19	15.26
Shmertmann [26]	CPT	16.55	9.91	26.46
European [27]	CPT	34.98	4.61	39.59
Cone-m [28]	CPT	20.86	9.72	30.58
LCPC [29]	CPT	12.09	7.36	19.45
Price & Wardle [30]	CPT	24.01	2.76	26.77
Unicone [31]	CPTu	24.38	8.48	32.86
Enhanced Unicone [32]	CPTu	39.07	6.49	45.56

After determining the bearing capacity of the piles by any of the proposed methods, the predicted value should be compared with the measured bearing capacity obtained from the dynamic pile tests (PDA). Hence, a new parameter is introduced as the model parameter, which is the ratio of the arithmetic average of the predicted bearing capacity obtained from different methods, ( $Q_p$ )<sub>ave</sub>, to the arithmetic averaged of the measured bearing capacity obtained from the pile dynamic tests, ( $Q_m$ )<sub>ave</sub>. Therefore, the model parameter for shaft, base, and ultimate bearing capacities in the end of driving (EOD), short-, medium- and long-term conditions, has separately been calculated for five test piles and 13 related PDA testing records.

Figs. (7-9) indicate the model parameter for shaft,  $Q_{sp(ave)}/Q_{sm(ave)}$ , base,  $Q_{bp(ave)}/Q_{bm(ave)}$ , and ultimate,  $Q_{up(ave)}/Q_{um(ave)}$ , bearing capacities in four time intervals, including end of driving (EOD), short-, medium- and long-term conditions. According to this parameter, those methods in which the model parameter values are above the standard line ( $Q_{p(ave)}/Q_{m(ave)} = 1$ ), propose upper estimates and in contrast, the methods in which the model parameter values are lower than the standard line, present the lower estimates.

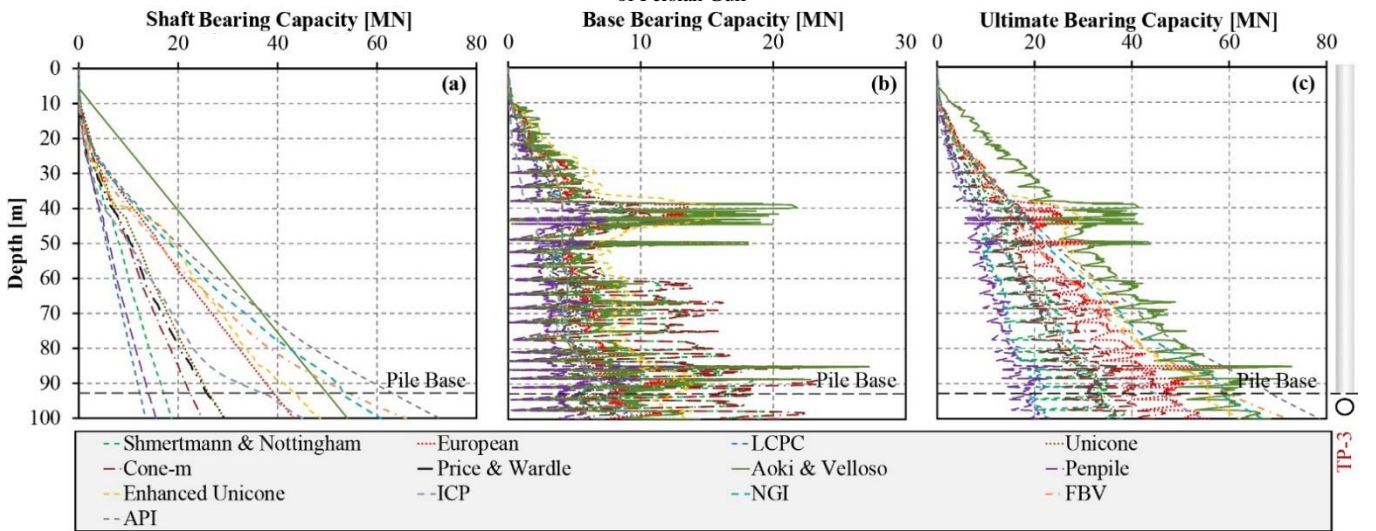


Fig. 6. Axial compressive bearing capacity curves obtained from different methods for: (a) shaft, (b) base, and (c) ultimate resistances related to TP-03.

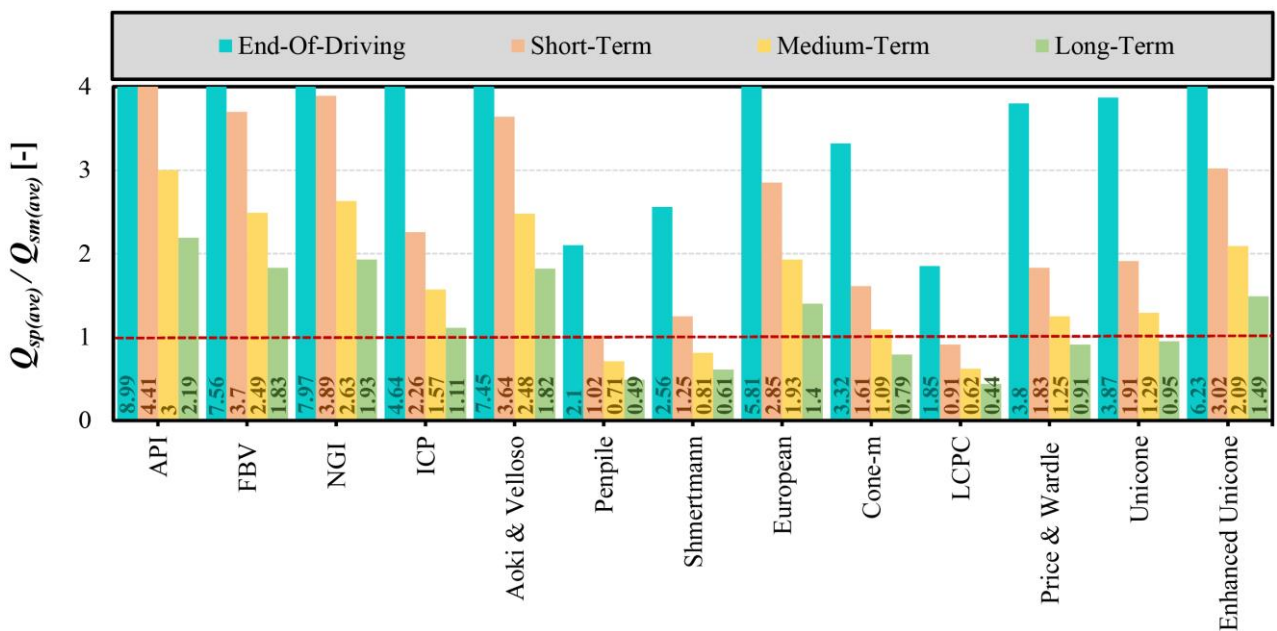


Fig. 7. The ratio of average predicted to average measured shaft bearing capacities,  $Q_{sp(ave)} / Q_{sm(ave)}$ , during time.

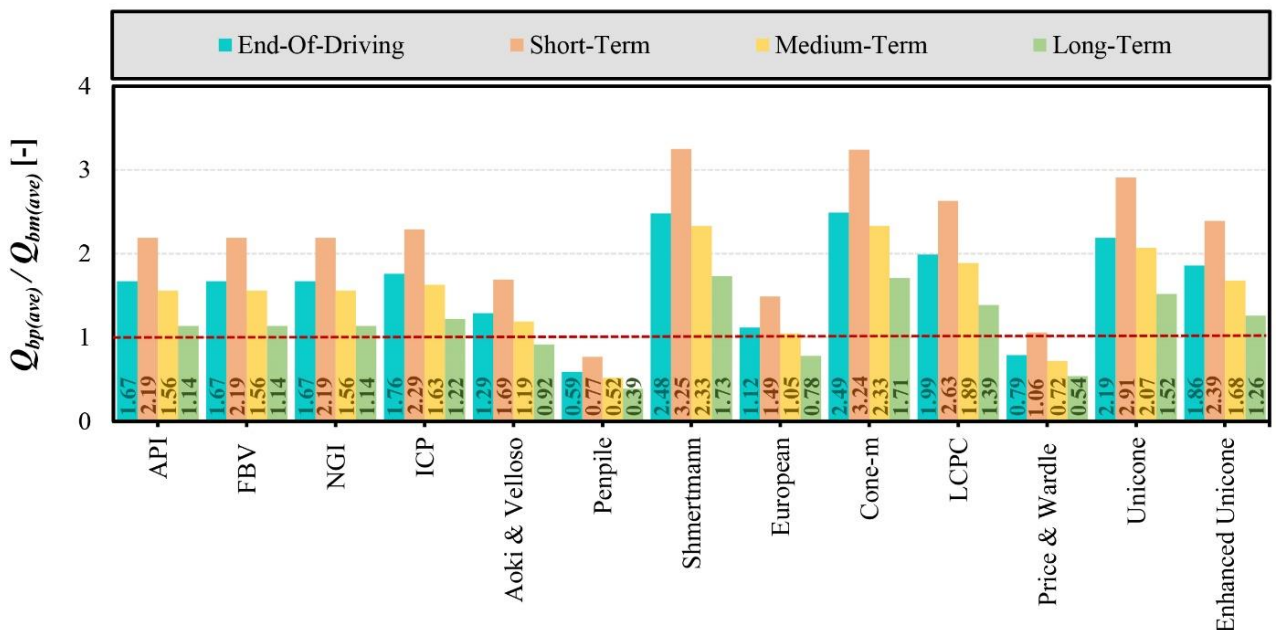


Fig. 8. The ratio of average predicted to average measured base bearing capacities,  $Q_{bp(ave)} / Q_{bm(ave)}$ , during time.

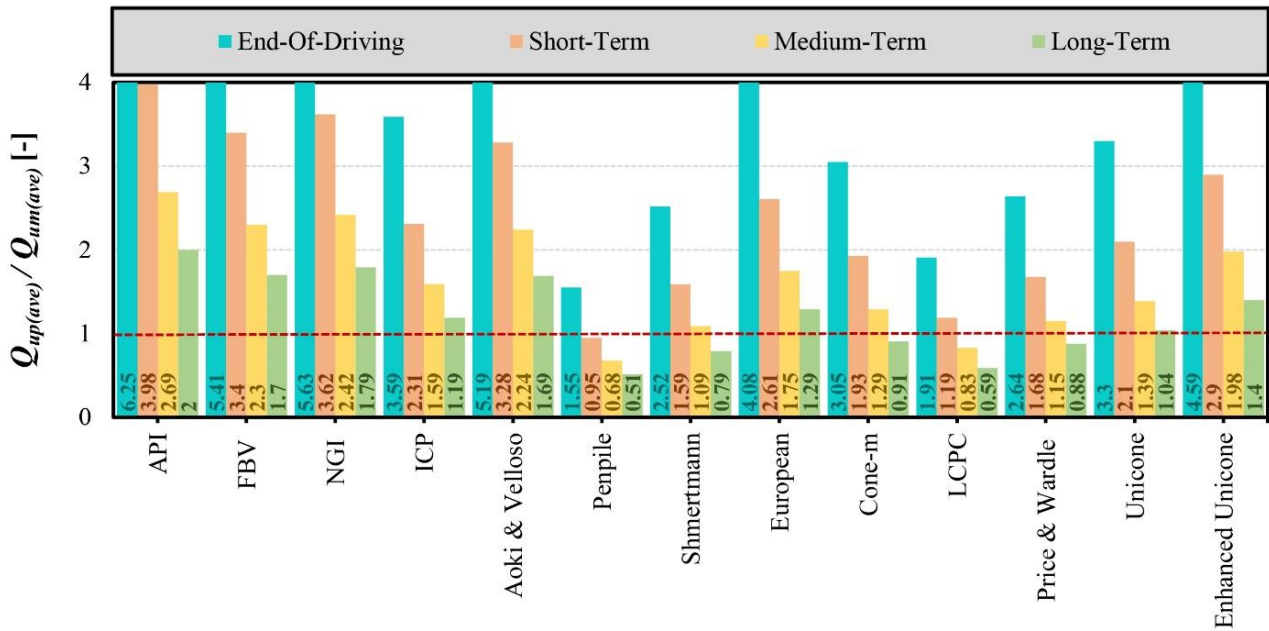


Fig. 9. The ratio of average predicted to average measured ultimate bearing capacities,  $Q_{up(ave)} / Q_{um(ave)}$ , during time.

#### 4. Results and Discussion

It is deduced that the pile bearing capacity is usually not a constant value, and it changes with time due to the soil set-up phenomenon. It is seen that the bearing capacities predicted by various methods can produce a wide range of results; therefore, each particular method cannot be accepted or rejected only based on the result of a pile test performed at one particular instance of time. According to the ratio of average predicted to average measured resistances  $(Q_p/Q_m)_{ave}$ , the closer the ratio is to 1, the more accurate the prediction. Therefore, for a proper presentation,  $\pm 10\%$  accuracy level around ratio 1 has been chosen to show the most accurate prediction methods. Fig. (10) presents those ratios of average predicted to average measured resistances  $(Q_p/Q_m)_{ave}$  that fall within the range between 0.90 and 1.10 in short-, medium- and long-term conditions. Given the fact that the closest results to 1 are the most desirable ones. As indicated in Figs. (7-9), Penpile [25], Price & Wardle [30] and again Penpile [25] methods in short-term condition, Cone-m [28], European [27] and Shmertmann [26] methods in medium-term condition, and finally, Unicone [31], Aoki & Velloso [24] and again Unicone [31] methods in long-term condition propose the best predictions among all methods for shaft, base, and ultimate bearing capacities, respectively.

As there will be often several months of time elapses between driving of piles and the completion of the super structure, piles will experience “time effects” on capacity before the actual design load is applied to the structure. As mentioned in Section 1, the main factors contributing to the time effect on the ultimate bearing

capacity of piles, particularly involved in the clayey soils, are reconsolidation and ageing. Due to time interval between pile driving and supper structure completion in offshore environment, the bearing capacity of piles increase with time. Therefore, the long-term bearing capacity of pile should be taken into account for pile design. It is worth noting that selecting short- and medium-terms bearing capacities for the design of offshore piles driven in clayey soils is significantly conservative. Consequently, long-term bearing capacity of these piles installed in clayey soils should be employed as a reference.

In order to evaluate the predictive performance and applicability of different methods in long-term condition, the calculated axial compressive bearing capacities of piles are compared with the PDA results recorded after 263 days from initial driving. As illustrated in Fig. (11), the methods with green and red columns are close to and far from the PDA 263-day BOR results, respectively. According to Fig. (11), Unicone [31], Price & Wardle [30], Aoki & Velloso [24] and Cone-m [28] methods propose the best predictions among all methods. In contrary, API [20], Aoki & Velloso [24], NGI [22], FBV [21], Penpile [25] and LCPC [29] present the worse consistency with the measured capacities in long-term condition. Fig. (11) also confirms that the API method shows the poorest performance and prediction quality, similar to the other static analysis methods. However, both CPT- and CPTu-based methods generally provide more reliable estimates of pile bearing capacity in clay than the static based-methods.

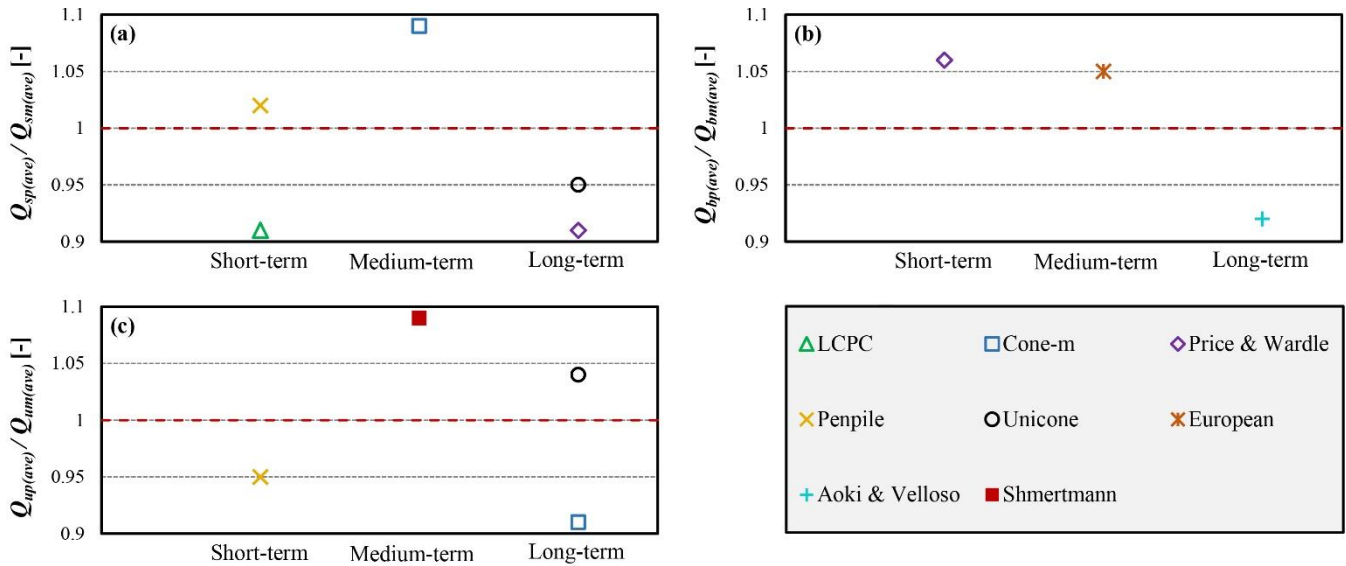


Fig. 10. The ratio of average predicted to average measured resistances,  $(Q_p/Q_m)_{ave}$ , in the range between 0.90 and 1.10 in short-, medium- and long-term conditions for: (a) shaft, (b) base and (c) ultimate bearing capacities.

### 5. Conclusions

This paper presents the axial compressive bearing capacities of the offshore piles driven in the Persian Gulf. The results have been calculated from nine CPT-based, two CPTu-based and four static-based analysis methods. Five well-documented long offshore steel pipe piles of the fixed offshore platforms (jackets) installed in the Persian Gulf with detailed PDA data measurements have been used to verify the prediction quality and the accuracy of each employed method. The measured data obtained from the field pile dynamic tests indicate that ultimate pile bearing capacity can increase around 320% over the nine months after initial driving. The average values of shaft, base, and ultimate bearing capacities obtained from the predictive methods have been compared to the average values measured by the field tests. In this regard, the model parameter,  $(Q_p/Q_m)_{ave}$  has been used to evaluate the prediction quality and the appropriateness of the given methods. The following conclusions are drawn from the current study:

- Soil set-up, which results in eventual increase in the pile bearing capacity, occurs in the marine clayey soils of the Persian Gulf.
- The shaft resistance experiences more alternation with time compared to the pile base resistance.
- The pile capacity increase with time in the Persian Gulf region is a function of the dissipation of excess pore water pressures developed during the pile driving.
- According to the pile driving analyzer (PDA) tests, the ratio of average ultimate bearing capacity obtained from the static analysis methods are 63%, 64%, 63% and 64% higher (e.g. over-predicted) than the corresponding ratios predicted by the CPT and CPTu-based

methods in end-of-driving, short, medium, and long-term conditions, respectively. This shows the acceptable accuracy of the CPT- and CPTu-based methods in comparison with the traditional static analysis methods. Therefore, the combination of CPT- or CPTu-based prediction method with the pile field test results can be considered by practicing engineers to estimate the axial bearing capacity of offshore piles.

- Investigations show that the proportion of the predicted pile bearing capacity by different CPT and CPTu-based methods to the measured pile capacity obtained from the pile driving analyzer (PDA) tests is in close agreement. Among the CPT- and CPTu-based methods, CPT prediction methods are more accurate rather than the CPTu prediction methods in short- and medium-term conditions. On the other hand, the bearing capacity predicted by the CPTu-based methods show more consistency with the measured capacities in the long-term condition.
- Long-term behavior of piles in clayey soils should be chosen as a reference for pile capacity due to time effects on the capacity of soil-pile system.
- Unicone (Eslami & Fellenius) [31], Aoki & Velloso [24] and Cone-m [28] methods show highest accuracy and appropriateness and in contrary, API method (static based-methods) show the lowest level of certainty against the measured capacities after 263 days of initial driving.

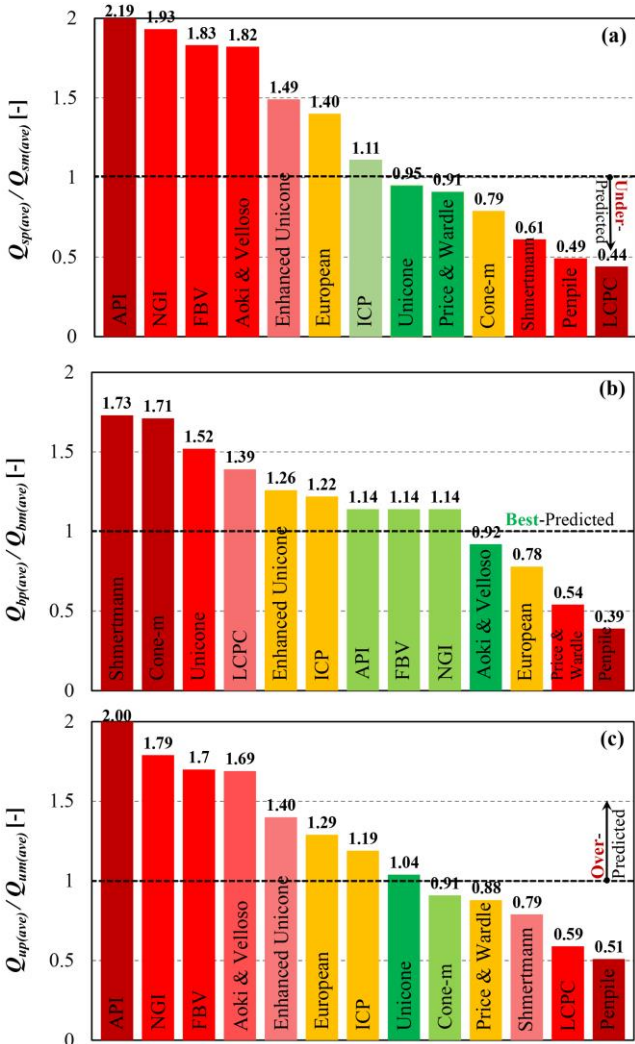


Fig. 11. Comparison between the ratio of average predicted to average measured resistances,  $(Q_b/Q_m)_{ave}$ , in long-term condition after 263 days for: (a) shaft, (b) base, and (c) ultimate bearing capacities.

### 6. Acknowledgment

The second author wants to express his sincere gratitude to the Iran's National Elites Foundation (INEF) for its moral support and encouragement.

### 7. List of symbols

- $a$  Net area ratio of a cone (Usually=0.80) [-]
- $A_b$  Cross section area of the pile base [m<sup>2</sup>]
- $A_r$  Area ratio [-]
- $b$  Loading direction coefficient [-]
- $C_b$  dimensionless coefficient for base [-]
- $C_s$  dimensionless coefficient for shaft [-]
- $D$  Outer diameter of pile [m]
- $d$  Inner diameter of pile [m]
- $e$  Base of natural logarithm ( $\approx 2.718$ ) [-]
- $F_b$  Empirical factors for base [-]
- $F_r$  Normalized friction ratio [%]
- $F_s$  Empirical factors for shaft [-]

- $f_s$  CPT Sleeve friction [MPa]
- $F_{tip}$  Base coefficient [-]
- $I_C$  CPT material index [-]
- $I_p$  Plasticity index [%]
- $K_c$  Radial effective earth pressure coefficient [-]
- $L$  Depth from the surface to the pile tip [m]
- $N_k$  Cone factor depending on local experience [-]
- $OCR$  Apparent over-consolidation ratio (called YSR by authors) [-]
- $P_{inn}$  Inner perimeter of pile [m]
- $P_{out}$  Outer perimeter of pile [m]
- $Q_{ann}$  Annulus capacity of pile [MN]
- $q_b$  Unite base bearing capacity of pile [MPa]
- $Q_b$  Base (or End) bearing capacity of pile [MN]
- $Q_{b,soil}$  Soil base capacity of pile [MN]
- $q_{ca(side)}$  Arithmetic average of  $q_c$  in a specific zone along the pile shaft [MPa]
- $q_{ca(tip)}$  Arithmetic average of  $q_c$  within 4D below and 8D above the pile tip [MPa]
- $q_{ca''(tip)}$  Arithmetic average of three cone tip resistance close to the pile tip [MPa]
- $q_{ca'''(tip)}$  Equivalent arithmetic average of  $q_c$  values of zone ranging from 1.5D below pile tip to 1.5D above pile tip [MPa]
- $q_{cd(tip)}$  Dutch average of  $q_c$  in an influence zone [MPa]
- $q_E$  Effective cone resistance [MPa]
- $q_{Eg}$  Geometric average of  $q_E$  values over the influence zone [MPa]
- $Q_{plug}$  Plug capacity of pile [MN]
- $q_s$  Unite shaft bearing capacity of pile [MPa]
- $Q_s$  Shaft bearing capacity of pile [MN]
- $Q_{s,inn}$  Inner frictional capacity of pile [MN]
- $q_t$  Corrected cone resistance [MPa]
- $Q_{tn}$  Normalized cone resistance (n varies with  $I_C$ ) [-]
- $Q_U$  Ultimate bearing capacity of pile [MN]
- $R^*$  Equivalent pile radius (For closed-ended piles, the radius  $R^*$  shall be replaced by  $R_{out}$ ) [m]
- $S_t$  Clay sensitivity [-]
- $S_u$  Undrained shear strength [kPa]
- $u_2$  Porewater pressure behind the cone [MPa]
- $z$  Depth from the surface to the point considered [m]
- $\alpha$  Adhesion factor [-]
- $\psi$  Normalized undrained shear strength [-]
- $\sigma'_{vo}$  Vertical effective overburden stress at depth  $z$  [MPa]
- $\sigma'_{rc}$  Local radial effective stress after full consolidation [MPa]
- $\sigma'_{rf}$  Radial effective stress at failure [MPa]
- $\delta'_f$  Soil-pile interface friction angle (depends upon  $I_p$ ) [°]

### 8. References

[1] Bullock, P.J., Schmertmann, J.H., McVay, M.C. and Townsend, F.C., "Side shear setup. I: Test piles driven in Florida", *Journal of*

- Geotechnical and Geoenvironmental Engineering*, Vol. 131(3), pp. 301-310, Mar 2005.
- [2] Bullock, P.J., Schmertmann, J.H., McVay, M.C. and Townsend, F.C., "Side shear setup. II: Results from Florida test piles", *Journal of Geotechnical and Geoenvironmental Engineering*, Vol. 131(3), pp. 301-310, Mar 2005.
- [3] Long, J. H., Kerrigan, J. A., and Wysockey, M. H. "Measured time effects for axial capacity of driven piling", *Journal of Transportation Research Record 1663*, pp. 57-63, 1999.
- [4] Tavenas, F., and Audy, R., "Limitations of the driving formulas for predicting bearing capacities of piles in sand", *Canadian Geotechnical Journal*, Vol. 9(1), pp. 47-62, Feb 1972.
- [5] Samson, L., and Authier, J., "Change in pile capacity with time: Case histories", *Canadian Geotechnical Journal*, Vol. 23(2), pp. 174-180, May 1986.
- [6] Zhang, M.Y., Liu, J.W., and Yu, X.X., "Field test study of time effect on ultimate bearing capacity of jacked pipe pile in soft clay", *Rock and Soil Mechanics*, Vol. 30(10), pp. 3005-3008, 2009.
- [7] Abu-Farsakh, M., Rosti, F., and Sourì, A. "Evaluating pile installation and subsequent thixotropic and consolidation effects on setup by numerical simulation for full-scale pile load tests", *Canadian Geotechnical Journal*, Vol. 52(11), pp. 1734-1746, 2015.
- [8] Komurka, V.E., Wagner, A.B. and Edil, T.B., "Estimating soil/pile set-up", *Wisconsin Highway Research Program*, Madison, WI, USA, Sep 2003.
- [9] Skov, R. a., and Denver, H., "Time-dependence of bearing capacity of piles", in *Proceedings of the 3rd International Conference on the Application of Stress-Wave Theory to Piles*, pp. 25-27, May 1988.
- [10] Axelsson, G., *Long-term set-up of driven piles in sand*, Institutionen för anläggning och miljö, Doctoral Thesis, 2000.
- [11] Long, J.H., Bozkurt, D., Kerrigan, J.A., and Wysockey, M.H., "Value of methods for predicting axial pile capacity", *Journal of the Transportation Research Board*, Vol. 1663(1), pp. 57-63, 1999.
- [12] Camp III, W.M., and Parmar, H.S., "Characterization of pile capacity with time in the cooper marl: study of application of a past approach to predict long-term pile capacity", *Journal of the Transportation Research Board*, Vol. 1663(1), pp.16-24, 1999.
- [13] Soderberg, L.O., "Consolidation theory applied to foundation pile time effects", *Geotechnique*, Vol. 11(3), pp. 217-225, Sep 1962.
- [14] Randolph, M.F., "Science and empiricism in pile foundation design", *Geotechnique*, Vol. 53(10), pp. 847-875, 2003.
- [15] Chow, F.C., Jardine, R.J., Nauroy, J.F. and Bruzy, F., "Time-related increases in the shaft capacities of driven piles in sand", *Geotechnique*, Vol. 47(2), pp. 353-361, 1997.
- [16] Randolph, M.F., Carter, J.P., and Wroth, C.P., "Driven piles in clay-the effects of installation and subsequent consolidation", *Geotechnique*, Vol. 29(4), pp. 361-393, 1979.
- [17] Eslami, A., Aflaki, E. and Hosseini, B., "Evaluating CPT and CPTu based pile bearing capacity estimation methods using Urmiyeh Lake Causeway piling records", *Scientia Iranica*, Vol. 18(5), pp. 1009-1019, 2011.
- [18] Ebrahimian, B., Movahed, V., and Nazari, A., "Soil characterisation of South Pars field", Persian Gulf, *Environmental Geotechnics*, Vol. 1(2), pp. 96-107, 2014.
- [19] Niazi, F.S. and Mayne, P.W., "Cone penetration test based direct methods for evaluating static axial capacity of single piles", *Geotechnical and Geological Engineering*, Vol. 31(4), pp. 979-1009, 2013.
- [20] American Petroleum Institute (API), "Recommended practice for planning, designing and constructing fixed offshore platforms – working stress design, RP2A-WSD", Washington, USA, 2007.
- [21] Kolk, H. J., and der Velde, E., "A reliable method to determine friction capacity of piles driven into clays", *Offshore Technology Conference*, Jan 1996.
- [22] Karlsrud, K., Clausen, C. J. F., and Aas, P. M., "Bearing capacity of driven piles in clay, the NGI approach", in *Proceedings of the International Symposium on Frontiers in Offshore Geotechnics*, Vol. 1, pp. 775-782, Sep 2005.
- [23] Jardine, R., Chow, F., Overy, R., and Standing, J., "ICP design methods for driven piles in sands and clays", Vol. 112, Mar 2005.
- [24] Aoki, N., and Velloso, D. D. A., "An approximate method to estimate the bearing capacity of piles", in *Proceedings of the 5th Pan-American Conference of Soil Mechanics and Foundation Engineering*, Vol. 1, pp. 367-376, 1975.
- [25] Clisby, M. B., Scholtes, R. M., Corey, M. W., Cole, H. A., Teng, P., and Webb, J. D., "An evaluation of pile bearing capacities", *Final Report, Mississippi State Highway Department*, Vol. 1, 1978.
- [26] Schmertmann, J. H., *Guidelines for cone penetration test: performance and design*, No. FHWA-TS-78-209. United States. Federal Highway Administration, Jul 1978.
- [27] De Ruiter, J., and Beringen, F. L., "Pile foundations for large North Sea structures", *Marine Georesources & Geotechnology*, Vol. 3(3), pp. 267-314, Jan 1979.
- [28] Tumay, M. T., and Fakhroo, M., "Friction pile capacity prediction in cohesive soils using electric quasi-static penetration tests", *Interim Research*, 1982.
- [29] Bustamante, M., and Gianceselli, L., "Pile bearing capacity prediction by means of static penetrometer CPT", in *Proceedings of the 2nd European symposium on penetration testing*, pp. 493-500, May 1982.
- [30] Price, G., and Wardle, I. F., "A comparison between cone penetration test results and the performance of small diameter instrumented piles in stiff clay", in *Proceedings of the 2nd European symposium on penetration testing, Amsterdam*, Vol. 2, pp. 775-780, 1982.
- [31] Eslami, A., and Fellenius, B. H., "Pile capacity by direct CPT and CPTu methods applied to 102 case histories", *Canadian Geotechnical Journal*, Vol. 34(6), pp. 886-904, Dec 1997.
- [32] Niazi, F.S. and Mayne, P.W., "CPTu-based enhanced UniCone method for pile capacity", *Engineering Geology*, 212, pp. 21-34, Sep 2016.

### 9. Appendix A

Several methods have been employed to predict the pile bearing capacity. Herein, the details of nine popular direct CPT and CPTu -based methods as well as the four static-based methods used in the paper are presented in Table A1.

**Table A1. Summary of static, CPT, and CPTu -based methods [8].**

Method [Reference]	Unit Shaft Resistance, $q_s$ [MPa]	Unit Base Resistance, $q_b$ [MPa]
<b>API Method [20]</b> (American Petroleum Institute, Gulf of Mexico, USA, 2007)	$q_s = \alpha S_u$ $\psi = \frac{S_u}{\sigma'_{V0}}$ For $\psi \leq 1.0$ ; $\alpha = 0.5 \psi^{-0.5} \leq 1.0$ For $\psi > 1.0$ ; $\alpha = 0.5 \psi^{-0.25} \leq 1.0$	$q_b = N_c S_u$ $N_c = 9$
Driven offshore piles, ( $\alpha$ -method)		
<b>FBV Method [21]</b> (Kolk & Van der Vlede, Fugro Engineers B.V., North Sea, 1996)	$q_s = \alpha S_u$ $\alpha = 0.9 \left(\frac{L-z}{D}\right)^{-0.2} \left(\frac{S_u}{\sigma'_{V0}}\right)^{-0.3} \leq 1.0$	$q_b = N_c S_u$
Driven piles, ( $\alpha$ -method)		
<b>NGI Method [22]</b> (Karlsrud et al., Norwegian Geotechnical Institute, North Sea, Norway, 2005)	For NC clays with $\psi < 0.25$ ; $q_s = \alpha^{NC} S_u$ $\alpha^{NC} = 0.32 (I_p - 10)^{0.3} \leq 1.0$ $0.20 < \alpha^{NC} < 1.00$	$q_b = N_c S_u$
	For OC clays with $\psi > 1.0$ ; $q_s = \alpha S_u F_{tip}$ $\alpha = 0.5 \psi^{-0.3} \leq 1.0$ $F_{tip (open)} = 1.0$ $F_{tip (closed)} = 0.8 + 0.2 \cdot \psi^{0.5}$ $1.00 < F_{tip (closed)} < 1.25$ For clays with $0.25 \leq \psi \leq 1.0$ ; $q_s = \alpha S_u$ $\alpha = 0.5 + (0.83 - 1.66 \alpha^{NC}) \log_{10} \psi \leq 1.0$ $q_s \text{ should be } \geq \beta_{Min} \sigma'_{V0}$ $\beta_{Min} = 0.06 (I_p - 12)^{0.33}$ $0.05 < \beta_{Min} < 0.20$	
Driven piles, ( $\alpha$ -method)		
<b>ICP Method [23]</b> (Jardine et al., Imperial Collage Pile, North Sea, UK & France, 2005)	$q_s = \sigma'_{rf} \tan \delta'_f$ $\sigma'_{rf} = 0.8 \sigma'_{rc}$ $\sigma'_{rc} = K_c \sigma'_{V0}$ $K_c = [2.2 + 0.016 OCR - 0.87 \log_{10}(S_t)] OCR^{0.42}$ $Max \left[ \left(\frac{L-z}{R^*}\right)^{-0.2} \cdot 8 \right]$ $R^* = (R_{out}^2 - R_{inn}^2)^{0.5}$	$q_b = N_c S_u$
Driven piles, ( $\beta$ -method)		
<b>Aoki &amp; Velloso Method [24]</b> (Aoki & De Alencar Velloso, 1975)	$q_s = \frac{q_{ca(side)} C_s}{F_s} \leq 120 \text{ kPa}$ $C_s (\%) \text{ depends on soil type: sand} = 1.4, \text{ silty sand} = 2.0, \text{ sandy silt} = 2.2, \text{ silt sand with clay or sandy clay} = 2.4, \text{ clay-sand-silt mix} = 2.8-3.0, \text{ clayey silt} = 3.4, \text{ silty clay} = 4.0, \text{ clay} = 6.0$ $F_s \text{ depends on pile type: bored} = 7.0, \text{ driven cast-in-situ} = 5.0, \text{ steel and precast concrete pile} = 3.5$	$q_b = \frac{q_{car(tip)}}{F_b} \leq 15 \text{ MPa}$ $F_b \text{ depends on pile type: bored} = 3.5; \text{ driven cast-in-situ} = 2.5, \text{ steel and precast concrete pile} = 1.75$
For piles in all soil types, (CPT-based method)		
<b>Penpile Method [25]</b> (Clisby et al., Mississippi State Highway Department, Mississippi, USA, 1978)	$q_s = \frac{f_s}{(1.5 + 14.47 f_s)}$ $q_s \text{ and } f_s \text{ are expressed in MPa}$	
For piles in all soil types, (CPT-based method)		

**Table A1. (Continued).**

Method [Reference]	Unit Shaft Resistance, $q_s$ [MPa]	Unit Base Resistance, $q_b$ [MPa]
<b>Shmertmann Method</b> [26]  (Nottingham & Shmertmann, Federal Highway Administration, Washington, USA 1975 & 1978)	In clay: $q_s = C_s f_s \leq 120 \text{ kPa}$ $C_s = 0.2 - 1.25$ as a function of $f_s$	$q_b = C_b q_{cd(tip)} \leq 15 \text{ MPa}$
	In sand: $q_s = C_s \left[ \sum_{z=0}^{8D} \frac{z}{8D} f_s + \sum_{z=8D}^L f_s \right] \leq 120 \text{ kPa}$ $C_s = 0.8 - 2.0$ as a function of $z/D$	$C_b$ is governed by over-consolidation ratio: $0.5 \leq C_b \leq 1.0$
For driven concrete, steel and timber piles in all soil types, (CPT-based method)		
<b>European Method</b> [27]  (de Ruiter & Beringen, North Sea, 1979)	In clay: $q_s = C_s s_{u(side)} \leq 120 \text{ kPa}$ For NC clay: $C_s = 1.0$ For OC clay: $C_s = 0.5$ $S_u = \frac{q_{c(side)}}{N_k}$ $15 \leq N_k \leq 20$	In clay: $q_b = N_c s_{u(tip)} \leq 15 \text{ MPa}$ $N_c = 9$ $S_u = \frac{q_{c(tip)}}{N_k}$ $15 \leq N_k \leq 20$
	In sand: $q_s = \text{Min} \left[ f_s, \frac{q_{c(side)}}{b} \cdot 120 \text{ kPa} \right]$ $b = 300$ for compression, and $= 400$ for tension	In sand: Similar to Shmertmann Method [14]
For offshore piles in all soil types, (CPT-based method)		
<b>Cone-m Method</b> [28]  (Tumay & Fakhroo, Louisiana Department of Transportation, USA, 1982)	$q_s = C_s f_s \leq 72 \text{ kPa}$ $C_s = 0.5 + 9.5 e^{(-90 f_s)}$ ; $f_s =$ Sleeve friction in MPa  $e = 2.718$	Similar to Shmertmann Method [14]
For all piles in clayey soils, (CPT-based method)		
<b>LCPC Method</b> [29]  (Bustamante and Gianceselli, French Highway Department, 1982)	$q_s = q_c / C_s < q_{smax}$	$q_b = C_b q_{ca'(tip)}$
	$C_s$ depending on soil type, pile type, and installation procedure: $30 \leq C_s \leq 150$	$C_b$ for non-displacement pile: clay and/or silt = 0.375, sand and/or gravel = 0.15, chalk = 0.20  $C_b$ for displacement pile: clay and/or silt = 0.60, sand and/or gravel = 0.375, sand and/or gravel = 0.40
For all pile types in all soil types, (CPT-based method)		
<b>Price &amp; Wardle Method</b> [30]  (Price & Wardle, London, UK, 1982)	$q_s = C_s f_s \leq 120 \text{ kPa}$	$q_b = C_b q_c \leq 15 \text{ MPa}$
	$C_s$ depending on pile type: driven = 0.53, jacked = 0.62, bored = 0.49	$C_b$ depending on pile type: driven = 0.35, jacked = 0.30
For jacked, driven and bored piles in stiff clayey soils, (CPT-based method)		
<b>Unicone Method</b> [31]  (Eslami & Fellenius, 142 pile load tests from 53 sites in 13 countries, 1997)	$q_s = C_s q_E$ $q_E = q_t - u_2$ $q_t = q_c - (1 - a) u_2$	$q_b = C_b q_{Eg}$
	$C_s$ (%) depending on soil classification chart derived from $q_t, f_s$ and $u_2$ [22]: soft sensitive soils = 8.0, Clay = 5.0, stiff clay and clay/silt mix = 2.5, silt and sand mix = 1.0, and sand = 0.4	$C_b$ for $D < 0.40 \text{ m} = 1.0$ $C_b$ for $D \geq 0.40 \text{ m} = \frac{1.0}{3D}$
For all pile types in all soil types, (CPTu-based method)		
<b>Enhanced Unicone Method</b> [32]  (Niazi & Mayne, 153 pile load tests from 52 sites in 17 countries, 2016)	$r_s = C_{se} q_E$ $C_{se} = \theta_1 \theta_2 \theta_3 C_{se(mean)}$	
	SBT <sub>n</sub> Zone 1: $C_{se(mean)} = 0.074 - 0.004 [Q_{tn} - 12 e^{(-1.4 F_r)}]$	
	SBT <sub>n</sub> Zones 2 to 9: $C_{se(mean)} = 10^{[0.732 (I_c) - 3.605]}$	
	$\theta_1$ depending on pile type: bored = 0.84; jacked = 1.02 and driven = 1.13	All SBT <sub>n</sub> Zones: $r_t = C_{te} q_{Eg}$ $C_{te(mean)} = 10^{[0.325 (I_c) - 1.218]}$
	$\theta_2$ depending on load direction: compression = 1.11 and tension = 0.85	
$\theta_3$ depending on loading rate: for $I_c \leq 2.6 = 1.00$ for $I_c > 2.6 = 0.97$ (stepped load), and 1.09 (constant rate of penetration)		
For all pile types in all soil types, (CPTu-based method)		